https://doi.org/10.1590/jatm.v15.1294 ORIGINAL PAPER

Experimental Investigation of the CFHT-27 Cusped-Field Hall Thruster Performance

Emin Saridede[1], Selcen Yediyildiz[1], Murat Celik[1,*]

1.Bogazici Universitesi – Department of Mechanical Engineering – Istanbul, Turkey.

*Correspondence author: murat.celik@boun.edu.tr

ABSTRACT

Cusped-field Hall thrusters (CFHT) have significant potential for use in many space missions due to their simplicity, long life and high efficiency. CFHT-27, designed and developed at the Bogazici University Space Technologies Laboratory (BUSTLab), is a prototype CFHT with a 27-mm diameter discharge channel. CFHT-27 utilizes samarium-cobalt (SmCo) permanent magnets. The thrust and efficiency of a cusped-field thruster is closely related to its size and design parameters. In this study, in order to understand the relationships between the design parameters and the thruster performance, the performance tests of the CFHT-27 are carried out for a given magnetic field topology. The thruster was operated at discharge voltages ranging from 250 to 500V with argon propellant with up to 3,000 s of specific impulse. The measurements show that CFHT-27 can achieve thrust values from 1 to 46 mN. Thus, this thruster can be used for a wide range of thrust values allowing throttle capabilities for different missions.

Keywords: Electric propulsion; Plasma thrusters; Thrust stand; Performance measurements.

INTRODUCTION

In recent years electric propulsion systems are increasingly being employed for the propulsive needs of satellites and spacecraft due to their much higher specific impulse levels when compared with chemical thrusters (Lev *et al.* 2019; Martinez-Sanchez and Pollard 1998, Mazouffre 2016). Among various electric propulsion concepts, Hall-effect thrusters are the most used electric thrusters (Lev *et al.* 2019). Hall-effect thrusters use electric and magnetic fields for both the ionization of the neutral propellant gas, hence creating a plasma, and the acceleration of the charged atoms of this plasma to produce thrust. In Hall thrusters, the imposed magnetic field affects both the electrons and the ions. However, due to their much larger masses, the ions move mostly unaffected by the magnetic field and are accelerated away from the thruster by the applied axial electric field, whereas the electrons follow an azimuthal trajectory that is perpendicular to both the applied axial electric field and the radial magnetic field (Martinez-Sanchez and Pollard 1998).

A cusped-field Hall thruster (CFHT) is a modified Hall thruster which was first studied by THALES Electron Devices in Germany (Koch *et al.* 2007; Kornfeld *et al.* 2003; 2007). This concept is also patented by Airbus Defence and Space GmbH (*Hey* et al. 2019). Based on the original design of THALES, researchers in academia have also investigated this thruster concept; at MIT (Courtney 2008; Courtney and Martinez-Sanchez 2007; Gildea *et al.* 2013; Matlock *et al.* 2010), at Stanford University (MacDonald *et al.* 2012), and at Harbin Institute of Technology (Liu *et al.* 2014a; b; Ma *et al.* 2015; Zhao *et al.* 2013). In this type of Hall thruster, unlike a single region of radial magnetic field of a typical Hall thruster, multiple regions of radial magnetic field are created by adopting alternating polarity permanent magnets. These radial magnetic field regions confine electrons that would normally move

Received: Oct 18, 2022 | **Accepted:** Feb 01, 2023
Section editor: José Atílio Fritz F Rocco
Peer Review History: Single-Blind Peer Review.

upstream to the anode. The electrons confined in the high radial magnetic field regions cause electron impact ionization of the neutral gas that is introduced to the discharge channel at the anode region. For these thrusters, due to the presence of multiple cusped regions, the discharge voltage can be much higher than that of a typical Hall thruster which only has a single cusped region (Courtney 2008; Kornfeld *et al.* 2006). Hence, in CFHTs, a wider range of thrust values can be obtained (Kornfeld *et al.* 2005). Furthermore, other researchers claimed that the cusped magnetic field in these thrusters can be effective in reducing the plasma wall interaction resulting in an increase in the thruster life (Gildea and Matlock 2013; Harmann *et al.* 2007).

Different studies have been conducted in order to understand the performance characteristics of CFHTs (Fahey *et al.* 2017; Hu *et al.* 2016; Liang *et al.* 2019). These characteristics have been investigated depending on the magnetic field strength in the discharge channel (Hu *et al.* 2016) or on key design parameters that are set to obtain maximum efficiency, thrust and I_{sp}. Four different configurations are analyzed for the permanent magnet rings with varying outer diameters. Results show that increasing magnetic field strength has a limiting effect on the radial cross-field electron current and it decreases the radial-width of the ionization region. Hence, the increase in the magnetic field strength reduces the propellant utilization as well as the performance of the thruster. It is also shown that the thrust and anode efficiency are positively affected in the case of weaker magnetic field strength in the discharge channel (Hu *et al.* 2016). Furthermore, an optimization with five different performance parameters are considered which include anode voltage, anode current, mass flow rate, magnet inner diameter and magnet outer diameter. For the anode current, an optimal value can be determined with the contribution of maximum anode potential and maximum mass flow rate. The results illustrate that the anode current and outer magnet radius have a significant effect on the performance. Regarding the location of the ionization regions, the differences in the discharge characteristics between cylindrical Hall thrusters and cusped-field thrusters using PIC-MCC simulations are investigated (Liang *et al.* 2019). The investigation indicates that the ionization regions of cusped-field thrusters move to the near-axis region and it has additional ionization in the plume region. In addition to these studies, also experimental measurements have been conducted on a divergent cusped-field thruster with a Faraday cup and a retarding potential analyzer to measure the ion current density and the ion energy distributions of the plume of the thruster (Gildea *et al.* 2013). The analyses show that the higher current density areas have more energetic and uniform ion groups. Nevertheless, it is also shown that these energetic ions are also thrown out at larger angles and cause an increase in the plume divergence. In the further stages of the plume measurements, different cathode operating conditions are set and it is found that the cathode and the thruster operating conditions are closely linked. Also, time dependent anode current measurements indicate a significant difference for the high and low-current operation modes of the thruster. It is seen that in the case of lower current operation modes, the anode current seems to be less oscillatory.

For the cylindrical Hall thruster, the ionization and acceleration regions are both near the anode and are coupled to each other (Raitses *et al.* 2010). However, for the cusped field thruster, the acceleration region and the ionization region are separated from each other. The cusped field thruster also has wider throttling ability due to lower anode electron energy deposition (Cui *et al.* 2018).

Previous research show that magnetic topology plays an important role in the performance and efficiency of CFHTs (Ma *et al.* 2015; Hu *et al.* 2016; Liang *et al.* 2019; Ma *et al.* 2013). In CFHTs, electrons emitted from the cathode reach the discharge channel and motion of the electrons are impeded by the cusped magnetic field regions. From the literature, a typical CFHT contains three radial magnetic field regions, which could be considered as the ionization regions. The first one is located at the exit plane of the thruster ionization chamber and the other two of these regions are located inside the ionization chamber. The optimal location of the two inner ionization regions is not very well understood. Hence in the literature the length between these ionization regions vary for different cusped-field thrusters (Koch *et al.* 2007; Courtney and Martinez-Sanchez 2007; MacDonald *et al.* 2012, Hu *et al.* 2016; Liang *et al.* 2019). Even though there are three separate cusped regions, the region at the exit of the cylindrical discharge chamber affects the divergence of the plume and a relatively lower number of electrons are trapped in this region. Because of that, the effective cusped regions are the ones inside the chamber. The topology of the exit magnetic cusp can be modified to control the plume divergence and can be used to increase thrust efficiency (Liu *et al.* 2014b).

For a CFHT, the paths of electrons are illustrated in Fig. 1, which shows the electrons leaving the cathode move upstream towards the positively biased anode. The presence of the cusp shaped radial magnetic field created by the permanent magnets impedes the motion of these backstreaming electrons creating an azimuthal electron current due to Hall effect in the regions of perpendicular electric and magnetic fields.

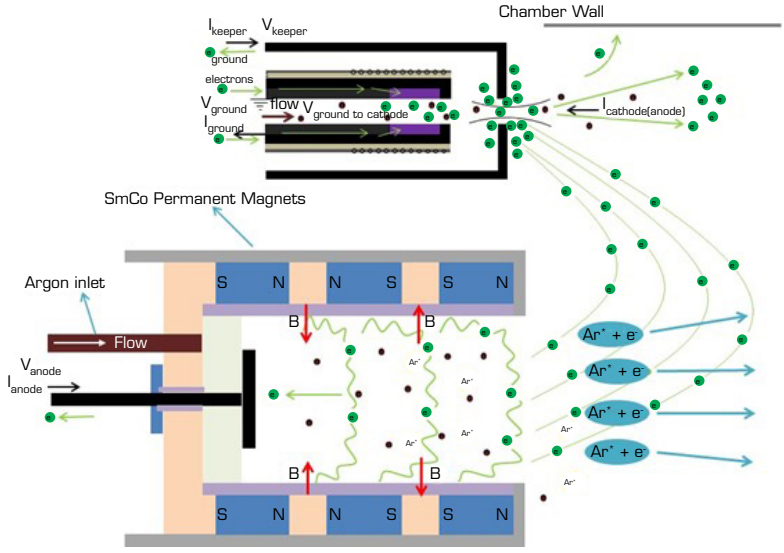

Source: Elaborated by the authors.

Figure 1. Schematic of the electron flow in a typical CFHT with double cusped region.

Based on the research presented in the literature, a prototype CFHT with a cylindrical discharge chamber diameter of 27 mm was designed and manufactured. The magnetic topology and the strength of the magnetic field is determined after a thorough review of the scientific literature in this field. Performance measurements of this thruster, called CFHT-27, are conducted inside the Bogazici University Space Technologies Laboratory (BUSTLab) vacuum chamber using an in-house built thrust stand. The operational parameters of the thruster were investigated for varying discharge voltage and propellant flow rate values. In this study, the range of thrust values that can be obtained with this thruster and its throttling ability, for determining its suitability for space mission, are investigated.

CFHT-27 CUSPED-FIELD HALL EFFECT THRUSTER

CFHT-27 has quartz discharge chamber walls. The 1.5-mm thick chamber walls has an inner diameter of 27 mm and an outer diameter of 30 mm. The thruster employs 6 mm thick axially polarized samarium-cobalt (SmCo) permanent ring magnets with an inner diameter of 30 mm and an outer diameter of 40 mm. Between the ring magnets 1018 steel spacers are used because of their high permeability at low cost compared to alternatives such as pure iron or Hiperco-50A. Similarly, for the base plate 1018 steel is used. An aluminum casing is used to protect the magnetic circuit and to hold the parts in place. A schematic of CFHT-27 is shown in Fig. 2.

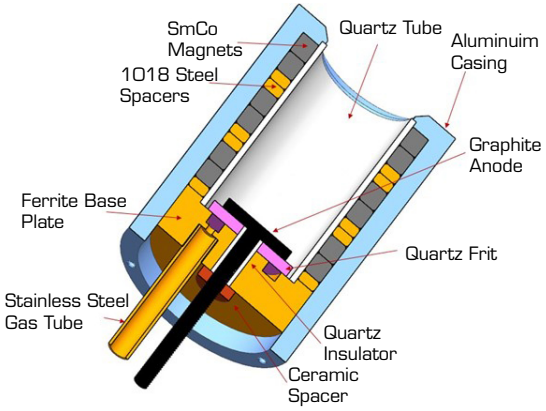

Source: Elaborated by the authors.

Figure 2. Schematic of CHFT-27 Hall effect thruster with materials used for each component.

The anode is made of graphite and is placed at the back wall. The diameter of the anode disc is 20 mm. The neutral gas enters the discharge channel through a 25-mm diameter porous quartz frit with a porosity of 100 microns. In most other similar cusped field thrusters, the propellant gas flows to the discharge chamber through the holes in the anode which is made of a conducting material (Ma *et al.* 2013; 2015; Peng *et al.* 2020). In the presented design, the porous nature of the quartz frit allows uniform distribution of neutral gas as it enters the discharge channel.

The CFHT-27 was operated using a LaB6 hollow cathode that is developed at BUSTLab (Kokal *et al.* 2021; Kurt *et al.* 2017). The cathode employs a 2-mm inner diameter, 4-mm outer diameter, LaB6 tube of 10 mm length placed inside a graphite cathode tube of 6 mm outer diameter 48 mm of length. The cathode is heated using a tantalum wire heater of a special design (Kurt *et al.* 2017). For the operation of the thruster, the exit orifice of the hollow cathode is located 22 mm axially and 38 mm radially away from the center point of the thruster exit plane. For the tests discussed in this paper, the cathode mass flow rate is set to 4 standard cubic centimeters per minute (sccm) and cathode keeper current is kept at 1.5 A.

For simulating the magnetic field topology, COMSOL Multiphysics AC/DC module was used. Since the magnets are permanent SmCo magnets, the physics is chosen to be magnetic fields, no currents and meshing is done with physics-controlled finer mesh. Considering the permanent magnets, magnetic flux conservation for each magnet is defined separately and the remanent flux densities are identified from the material properties of SmCo and this value is given as 1.05 Tesla. Figure 3 shows the magnetic field topology of CFHT-27. Effect of the magnets closest to the discharge chamber exit plane on the magnetic field lines in the plume region magnetic topology are observed closely, since the magnetic field lines in this region direct the electrons flowing from the cathode to the discharge channel.

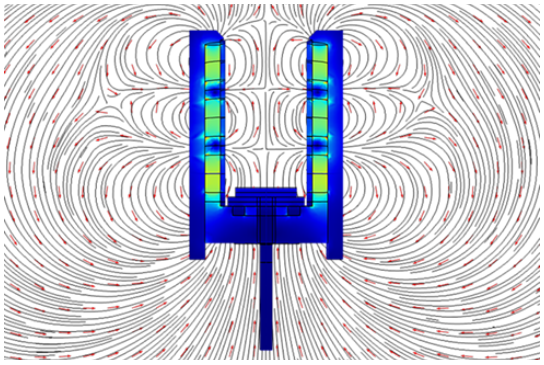

Source: Elaborated by the authors.

Figure 3. Magnetic field topology of CFHT-27.

The 2-2-2 magnetic field configuration is investigated for the SmCo permanent magnets and ferrite spacers. The magnetic topology results are presented in this study. In this configuration, the green parts are the SmCo magnets and the blue spaces in between are the ferrite spacers. One can observe that there are two separatrix lines between the cusped regions. These cusped regions are for the sufficient ionization of the gas. The cathode is placed along the diverging plume at the magnetic field lines along the exit of the thruster but not close to the main separatrix region, which is directly in the middle of the thruster. Nearly no divergence is observed for the 2-2-2 configuration in the middle part of the thruster. However, the magnet configurations can be changed to decrease the plume divergence at the outer exit in further study, since this leads to a decrease in the thrust because of the thrust vector. The magnetic field strength in a given stage increases as the total length of that magnet stage is increased. In the configuration presented in Fig. 3, the magnetic field strength at the cusp regions goes up to 1400 Gauss. A more detailed report about the effect of alternative magnetic field topology configurations and the strength at the exit to decrease the plume divergence will be presented as a separate study in the future.

EXPERIMENTAL MEASUREMENTS AND DISCUSSION

The tests of the CFHT-27 are conducted inside the BUSTLab vacuum chamber, which is 1.5 m in diameter and 2.7 m in length (Korkmaz *et al.* 2015). The picture of the BUSTLab vacuum chamber used for the tests of the CFHT-27 is shown in Fig. 4. During the tests, the pressure inside the vacuum chamber was 6.2×10^{-5} torr when operating the thruster at 17 sccm anode flow

and 4 sccm cathode flow of argon propellant. Picture from the tests of the thruster is shown in Fig. 5. The plume divergence angle decreases, when the separatrix gets a slope perpendicular to the direction of the electric field created due the anode voltage (Ma *et al.* 2015; Zhurin *et al.* 1999). Based on the discussion from the literature, the main plasma regions are between the bright edges of the plume regions (Ma *et al.* 2015). Thus, the region between the bright edges of the plume can be considered as the main ion beam region. From the visual inspection of the plume, the divergence angle is estimated to be about 32°.

Source: Elaborated by the authors.

Figure 4. BUSTLab vacuum chamber.

Source: Elaborated by the authors.

Figure 5. Picture of CFHT-27 in operation inside the vacuum chamber.

Thrust Measurements

As mentioned before, thrust measurements of the CFHT-27 were conducted using in-house built inverted pendulum type thrust stand (Kokal and Celik 2017a; b). The resolution for the thrust measurements was ± 0.296 mN. The thrust stand system uses a Linear Variable Differential Transformer (LVDT) sensor to measure the displacement of the inverted pendulum structure due to the force produced by the thruster. This displacement information with the premeasured stiffness value of the system gives the created thrust value. The thrust is measured in such a way that the LVDT displacement value is recorded when the anode voltage, hence the electric field, is applied. Thus, thrust due to the momentum of the Argon gas before the application of the voltage to the anode is accounted separately. Since the BUSTLab vacuum chamber employs cryogenic pumps for keeping the chamber background pressure at reasonably low levels during the thruster's operation, perturbations caused by the operation of the cryopumps cause noise during LVDT signal data reading. Because of that for certain thrust measurements, the cryopumps were turned off for short periods of time without affecting the pumping capacity and hence the chamber background pressure.

The measured thrust levels versus the applied anode voltage for various flow rates are shown in Fig. 6. As expected, with increasing anode voltage the generated thrust increases. This is expected, as the ions are accelerated to higher exit velocities. In addition to the increased ion exit velocities, increase of anode voltage would also increase the rate of ionization inside the ionization chamber of the thruster due to increase in the frequency of ionization collisions with the increase of both in the temperature of electrons

as well as the energy of the created ions. Similarly, increase in the propellant flow rate to the anode results in increased thrust. As the flow rate is increased, the slope of the thrust versus anode voltage line shows slight increase. Figure 7 shows the measured thrust levels versus the propellant flow rate to the anode for various anode voltages. As seen in this figure, the slope of the thrust versus anode flow rate curve becomes steeper as the applied anode voltage is increased. Hence, at higher applied anode voltages, the range of thrust values that can be obtained becomes wider, as seen in Fig. 7.

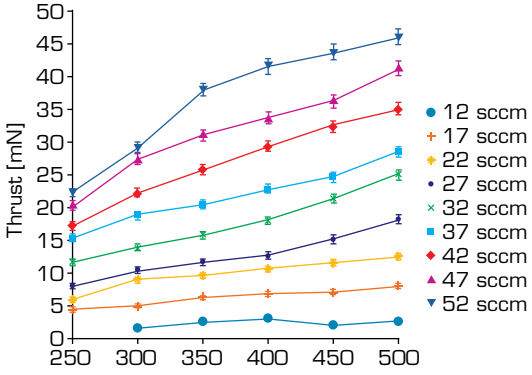

Source: Elaborated by the authors.

Figure 6. CFHT-27 thrust versus anode voltage.

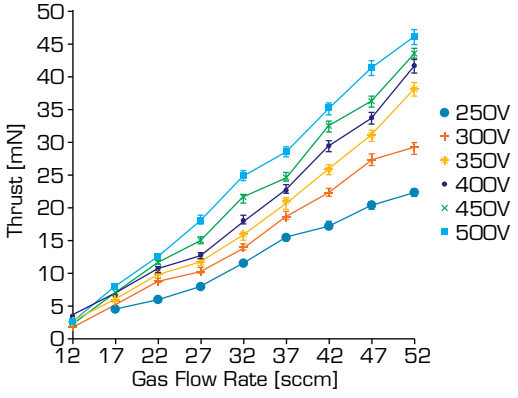

Source: Elaborated by the authors.

Figure 7. CFHT-27 thrust versus anode flow rate.

Based on the measured anode current and thrust values, the anode efficiency, η_{anode}, is calculated using:

$$\eta_{anode} = \frac{T^2}{2\dot{m}_a V_a I_a} \tag{1}$$

where T is the measured thrust, $\dot{m}_a$ is the set anode mass flow rate, V_a is the set anode voltage and I_a is the measured anode current. Similarly, the specific impulse of anode only, I_{sp} is calculated using:

$$I_{sp} = \frac{T}{\dot{m}_a g} \tag{2}$$

where g is the earth's specific gravity.

In Fig. 8, the general behavior of the anode current, anode power, specific impulse of anode only, I_{sp} , and the anode efficiency, η_{anode}, versus applied anode voltage can be seen for varying anode propellant flow rate. Similarly, in Fig. 9 the same performance characteristics are presented versus the anode propellant flow rate for varying applied anode voltage. In Fig. 8a, it is seen that the anode current remains almost constant for varying anode voltages for a set anode flow rate value. As the anode flow rate increases, the anode current increases, as

would be expected. On the other hand, Fig. 9a shows that the change in the anode voltage has a small effect on the anode current for a set of anode propellant flow rate value valves whereas the increase in the discharge current is almost linear with the change in the flow rate.

As seen in Figs. 8b and 9b, the power increases with increasing anode flow rate, and this increase is steeper for higher flow rates. As seen from these figures that this thruster has been operated at a very wide range of power values. The calculated I_{sp} values, except for the 12 sccm flow rate are shown in Figs. 8c and 9c. As expected, the specific impulse increases for increased anode voltage. The observed I_{sp} values vary between 500 to above 3,000 s, indicating a wide range of propellant utilization efficiency levels for varying discharge voltage and propellant flow rate values. With the selection of an appropriate I_{sp} value, hence appropriate discharge voltage and propellant flow rate, a better performance can be expected from CFHT-27. This feature can be important when making decision on what type of a mission a specific thruster would be suitable for.

As shown in Fig. 8d, CFHT-27 displays a general trend of increasing efficiency with increasing anode voltage. Thus, the figure shows that as the anode voltage is increased, the thruster performance increases. This is an expected result since as the discharge voltage is increased the ionization rate increases which improves the anode efficiency. Similarly, Figure 9d shows that as the anode flow rate increases the efficiency increases. The relationship between the thrust and the anode propellant flow rate is almost linear. Hence, it can be inferred from the figures that the flow rate where the leveling of the measured thrust was not reached in the scope of the experiments conducted as part of this study. The flow rates where the thrust value levels off must be at higher flow rates, hence it can be inferred that the thruster can handle higher flow rates and hence higher thrust values. Therefore, a wide working range thrust values than measured as part of this study can be expected from this thruster making it a suitable candidate for a wider range of space missions.

Figures 8d and 9d show that the efficiency tends to increase with increasing anode flow rate. These two graphs can point that CFHT-27 can produce higher thrust values, and again this would widen the range of thrust values and hence its usage. It is a desired result for CFHT-27, because even if it is a small thruster in size, it can be used in a wider range of space missions than would be expected for such a small thruster. It is observed that for higher discharge voltages the efficiency is also improved, hence a higher performance thruster is achieved.

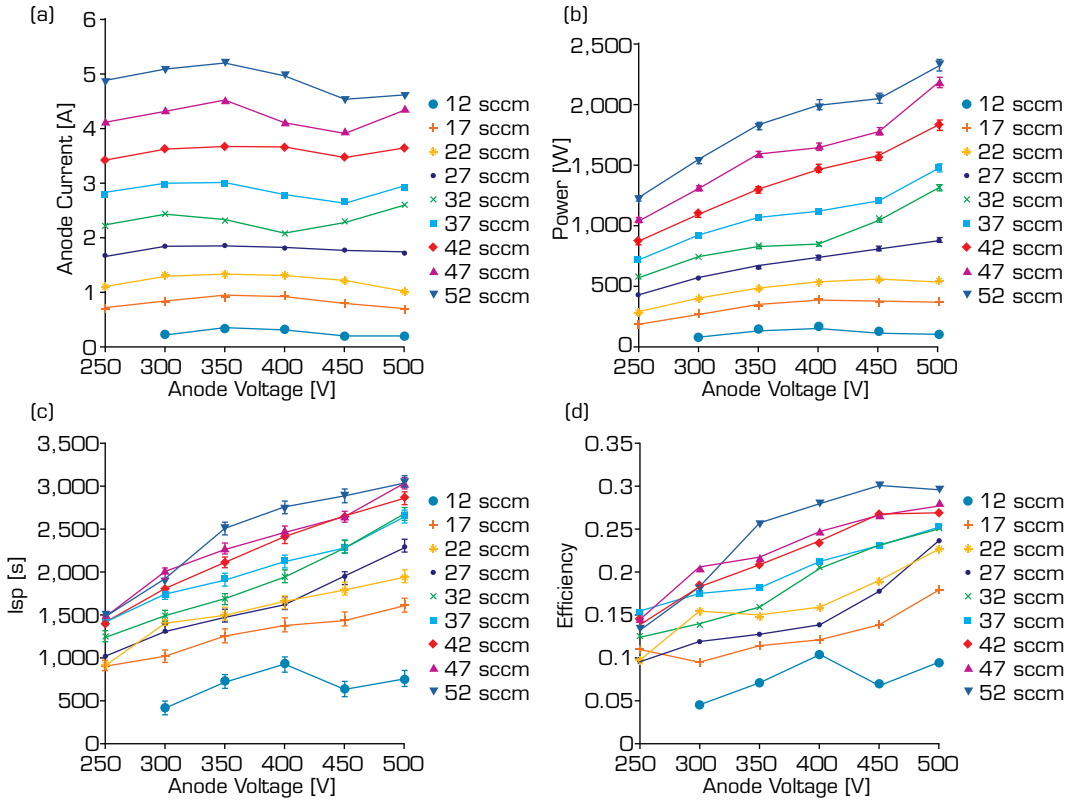

Figure 8. CFHT-27 performance measurement results for varying anode voltage rate values. (a) Anode current versus anode voltage, (b) Anode power versus anode voltage, (c) Anode specific impulse versus anode voltage, (d) Anode efficiency versus anode voltage.

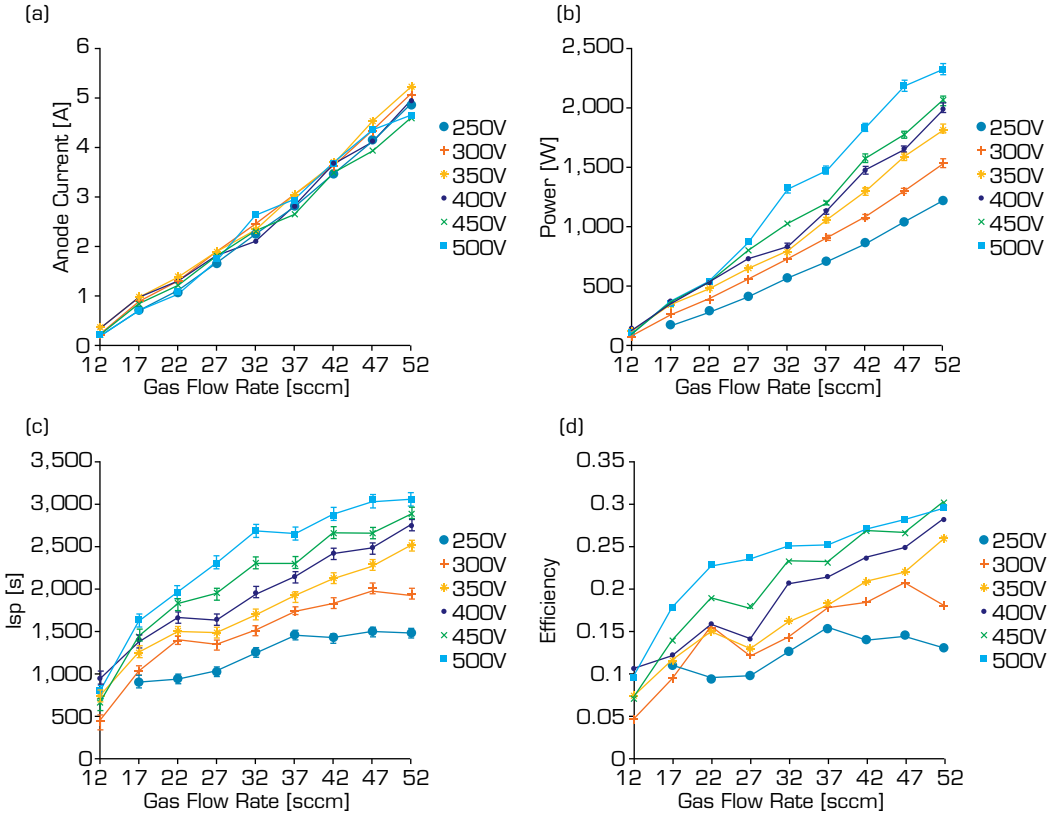

Figure 9. CFHT-27 performance measurement results for varying anode flow rate values. (a) Anode current versus anode flow rate, (b) Anode power versus anode flow rate, (c) Anode specific impulse versus anode flow rate, (d) Anode efficiency versus anode flow rate.

As seen in Fig. 8b and Fig. 7, as the flow rate increases the anode current and the thrust increase. For the configuration tested in this report, for 52 sccm anode flow rate at 500 V discharge voltage, the measured thrust is 46 mN corresponding to a specific impulse of 3,037 s at an anode power of 2,320 W with 29.6% anode efficiency. As observed, the increase in the anode flow rate increases the thrust; however, if the flow rate is further increased, after a certain flow rate it is expected that the rate of increase in thrust will drop.

In addition to changing the anode voltage and the anode flow rate for the investigation of the performance of this thruster, via altering the magnetic topology and the separatrix angle at the cusped region near the exit plane of the discharge chamber a better performance characteristic can be found. However, the focus of this study was limited to presenting a predetermined magnetic field topology and alteration to magnetic field topology is left as a separate study.

CONCLUSION

This paper presents the performance measurements of the CFHT-27 for a predetermined magnetic field topology. The thruster was operated using Argon as the propellant. During the tests, the anode flow rate was varied from 12 to 52 sccm with 5 sccm increments and the discharge voltage was varied from 250 to 500 V with 50 V increments. The measured thrust values have a wide range from 1 to 46 mN indicating an almost continuous range of thrust values obtainable for this thruster. Such a wide range of thrust values at reasonable anode efficiency values make this thruster an attractive candidate for space missions where high throttleability is desired.

A more detailed report about the effect of alternative magnetic field topology configurations will be presented as a separate study in the future.

CONFLIT OF INTEREST

Nothing to declare.

AUTHORS' CONTRIBUTION

Conceptualization: Saridede E, Yediyildiz S and Celik M; **Methodology**: Saridede E and Celik M; **Software** Saridede E; **Validation**: Saridede E; **Formal analysis**: Saridede E and Yediyildiz S; **Investigation**: Saridede E, Yediyildiz S and Celik M; **Resources**: Saridede E and Celik M; **Data Curation**: Saridede E and Celik M; **Writing – Original Draft**: Saridede E, Yediyildiz S and Celik M; **Writing – Review & Editing**: Saridede E and Celik M; **Visualization**: Saridede E and Yediyildiz S; **Supervision**: Celik M; **Project administration**: Celik M; **Funding acquisition**: Celik M.

DATA AVAILABILITY STATEMENT

The data will be available upon request.

FUNDING

Scientific and Technological Research Council of Turkey
[https://doi.org/10.13039/501100004410]
Grant No: 214M572

ACKNOWLEDGEMENTS

Not applicable.

REFERENCES

Courtney DG (2008) Development and characterization of a diverging cusped field thruster and a lanthanum hexaboride hollow cathode (master's thesis). Cambridge: Massachusetts Institute of Technology. [accessed May 5 2022]. http://hdl.handle.net/1721.1/45239

Courtney DG, Martinez-Sanchez M (2007) Diverging cusped-field Hall thruster (DCHT). Paper presented Proceedings 30th International Electric Propulsion Conference. Florence, Italy.

Cui K, Liu H, Jiang WJ, Sun QQ, Hu P, Yu DR (2018) Effects of cusped field thruster on the performance of drag-free control system. Acta Astronaut 144:193-200. https://doi.org/10.1016/j.actaastro.2017.12.032

Fahey T, Muffatti A, Ogawa H (2017) High fidelity multi-objective design optimization of a downscaled cusped field thruster. Aerospace 4(4):55. https://doi.org/10.3390/aerospace4040055

Gildea SR, Matlock TS, Martínez-Sánchez M, Hargus Jr WA (2013) Erosion measurements in a low-power cusped-field plasma thruster. J Propuls Power 29(4):906-918. https://doi.org/10.2514/1.B34607

Harmann HP, Koch N, Kornfeld G (2007) Low complexity and low cost electric propulsion system for telecom satellites based on HEMP thruster assembly. Paper presented Proceedings of the 30th International Electric Propulsion Conference. Florence, Italy.

Hey FG, Johann U, Kornfeld G (2019) Cusped-field thruster, US Patent 10,184,460.

Hu P, Liu H, Gao Y, Yu D (2016) Effects of magnetic field strength in the discharge channel on the performance of a multi-cusped field thruster. AIP Advances 6(9):095003. https://doi.org/10.1063/1.4962548

Koch N, Harmann H, Kornfeld G (2007) Status of the THALES high efficiency multi stage plasma thruster development for HEMP-T 3050 and HEMP-T 30250. Paper presented Proceedings of the 30th International Electric Propulsion Conference. Florence, Italy.

Kokal U, Celik M (2017a) Development of a mili-Newton level thrust stand for thrust measurements of electric propulsion systems. Paper presented 2017 8th International Conference on Recent Advances in Space Technologies (RAST). IEEE; Istanbul, Turkey. https://doi.org/10.1109/RAST.2017.8002970

Kokal U, Celik M (2017b) Development of BUSTLab thrust stand for mili-Newton level thrust measurements of electric propulsion systems. Paper presented 35th International Electric Propulsion Conference. Atlanta, GA, USA.

Kokal U, Turan N, Celik M (2021) Thermal analysis and testing of different designs of LaB6 hollow cathodes to be used in electric propulsion applications. Aerospace 8(8):215. https://doi.org/10.3390/aerospace8080215

Korkmaz O, Jahanbakhsh S, Celik M, Kurt H (2015) Space propulsion research vacuum facility of the Bogazici University Space Technologies Laboratory. Paper presented 2015 7th International Conference on Recent Advances in Space Technologies (RAST). IEEE; Istanbul, Turkey. https://doi.org/10.1109/RAST.2015.7208420

Kornfeld G, Harmann HP, Koch N (2005) Status and limited life test results of the cylindrical HEMP 3050 thruster. Paper presented 41st AIAA/ASME/SAE/ASEE Joint Propulsion Conference & Exhibit. AIAA; Tucson, AZ, USA. https://doi.org/10.2514/6.2005-4223

Kornfeld G, Koch N, Coustou G (2003) First test results of the HEMP thruster concept. Paper presented Proceedings of the 28th International Electric Propulsion Conference, 2003.

Kornfeld G, Koch N, Harmann HP (2007) Physics and evolution of HEMP-thrusters. Paper presented Proceedings of the 30th International Electric Propulsion Conference, Florence, Italy.

Kornfeld G, Koch N, Harmann HP, Micheli P, Meusemann H, Gengembre E (2006) High power HEMP-thruster module, status and results of a DLR and ESA development program. Paper presented 42nd AIAA/ASME/SAE/ASEE Joint Propulsion Conference & Exhibit. AIAA; Sacramento, CA, USA. https://doi.org/10.2514/6.2006-4476

Kurt H, Kokal U, Turan N, Celik M (2017) Note: Coaxial-heater hollow cathode. Rev Sci Instrum 88(6):066103. https://doi.org/10.1063/1.4986111

Lev D, Myers RM, Lemmer KM, Kolbeck J, Koizumi H, Polzin K (2019) The technological and commercial expansion of electric propulsion. Acta Astronaut 159:213-227. https://doi.org/10.1016/j.actaastro.2019.03.058

Liang S, Liu H, Yu D (2019) Effect of magnetic field configuration on discharge characteristics in permanent magnet thrusters with cusped field. Paper presented 36th International Electric Propulsion Conference. Vienna, Austria.

Liu H, Sun G, Zhao Y, Chen P, Ma C, Wu H, Yu D (2014a) Plume control of a cusped field thruster. IEEE Trans Plasma Sci 43(1):127-129. https://doi.org/10.1109/TPS.2014.2360015

Liu H, Wu H, Zhao Y, Yu D, Ma C, Wang D, Wei H (2014b) Study of the electric field formation in a multi-cusped magnetic field. Phys Plasmas 21(9):090706. https://doi.org/10.1063/1.4896250

Ma C, Liu H, Hu Y, Yu D, Chen P, Sun G, Zhao Y (2015) Experimental study on a variable magnet length cusped field thruster. Vacuum 115:101-107. https://doi.org/10.1016/j.vacuum.2015.02.007

Ma C, Liu H, Yu D, Zhao Y, Chen P, Sun G (2013) Experiment research on a variable magnet length cusped field thruster. Paper presented 33rd International Electric Propulsion Conference. Washington, DC, USA.

MacDonald N, Young C, Cappelli M, Hargus Jr WA (2012) Ion velocity and plasma potential measurements of a cylindrical cusped field thruster. J Appl Phys 111(9):093303. https://doi.org/10.1063/1.4707953

Martinez-Sanchez M, Pollard JE (1998) Spacecraft electric propulsion – an overview. J Propuls Power 14(5):688-699. https://doi.org/10.2514/2.5331

Matlock T, Gildea SR, Hu F, Becker N, Lozano P, Martinez-Sanchez M (2010) Magnetic field effects on the plume of a diverging cusped-field thruster. Paper presented 46th AIAA/ASME/SAE/ASEE Joint Propulsion Conference & Exhibit. Nashville, TB, USA. https://doi.org/10.2514/6.2010-7104

Mazouffre S (2016) Electric propulsion for satellites and spacecraft: established technologies and novel approaches. Plasma Sources Sci Technol 25(3):033002. https://doi.org/10.1088/0963-0252/25/3/033002

Peng H, Daren Y, Yan S (2020) Magnet stage optimization of 5 kW multi-cusped field thruster. Plasma Sci Technol 22(9):094015. https://doi.org/10.1088/2058-6272/aba680

Raitses Y, Merino E, Fisch NJ (2010) Cylindrical Hall thrusters with permanent magnets. J Appl Phys 108(9):093307. https://doi.org/10.1063/1.3499694

Zhao Y, Liu H, Yu D, Ma C (2013) Particle-in-cell simulations for a variable magnet length cusped-field thruster. Paper presented Proceedings 31st International Electric Propulsion Conference.

Zhurin VV, Kaufman HR, Robinson RS (1999) Physics of closed drift thrusters. Plasma Sources Sci Technol 8(1):R1. https://doi.org/10.1088/0963-0252/8/1/021